SemantJournals

American Journal of Technology Advancement 2997-9382, Vol 03, No. 5, 2026

Article

Wave-Induced Longshore Currents, Sediment Transport and Bay-Entrance Siltation in Unsteady-Flow Mountain Reservoirs: A Hydraulic Method Validated at the Hisorak Reservoir, Uzbekistan

Ashraf R. Rakhimov
University of Economics and Pedagogy Karshi, Uzbekistan
ashrafrhmv@gmail.com

Abstract: Reservoir banks, slopes and the entrances of sheltered bays undergo progressive deformation driven by wind-induced waves and the alongshore currents they generate, threatening the safety, navigability and effective storage of water-supply facilities. This study develops and validates a hydraulic method for predicting wave-induced longshore currents, bank reformation and bay-entrance siltation in unsteady-flow mountain reservoirs, using the Hisorak Reservoir on the Aksu (Akdarya) River (Kashqadarya Province, Uzbekistan) as a case study. The mean longshore current velocity is obtained from a water-mass continuity model of the surf zone that expresses the velocity through the wave celerity and the wave-approach angle, requiring a single surf measurement rather than simultaneous deep-water observations. A longshore sediment-transport relation and a one-line entrance-width model close the scheme, and a shift of the wave breaking point by the current is incorporated to correct the approach angle at oblique incidence. The model predicts that both the maximum alongshore velocity and the maximum entrance siltation occur when the wind acts at about 45° to the shoreline, in agreement with independent field evidence. Validation against nearshore current measurements yields a mean deviation of 11.6 %, and the method reproduces the multi-year narrowing of a bay entrance under repeated clearance. A transverse sediment-retaining structure, dimensioned with the method, reduces the predicted entrance siltation by about two-thirds, extending the clearance interval several-fold. The approach provides a transparent, field-economical basis for forecasting deformation and dimensioning bank protection at arid-zone mountain reservoirs.

Keywords: reservoir deformation; longshore current; wave-induced flow; bank erosion; bay-entrance siltation; sediment transport; sediment-retaining structure; Hisorak Reservoir.

This is an open-access article under the CC-BY 4.0 license

1. Introduction

Wind-driven motion in the coastal zone is one of the principal agents reshaping reservoir shores. Alongshore currents with velocities reaching 1.5 m s^{-1} and above, generated by wind stress and by the energy released in the breaking-wave zone, erode unprotected banks and transport large

volumes of sediment toward intakes, inlets and the entrances of sheltered bays. Where the longshore drift converges, sediment is deposited across a bay entrance; the resulting spit grows, merges and progressively isolates the bay from the open water body. Repeated mechanical clearance of these entrances is labour-intensive and costly, and the entrances re-silt within a few years of each intervention[1].

The quantitative description of these currents and of the sediment they carry therefore underpins the design of water intakes, harbours, wave-damping and bank-protection structures. Classical treatments of wind waves and bank reformation on lowland reservoirs, the energetic theory of alongshore currents and radiation-stress longshore-current theory provide the physical foundation. Two gaps, however, persist for the practitioner working on mountain reservoirs. First, most velocity-prediction schemes require the reliable determination of bottom friction and lateral turbulent stresses, or simultaneous in-situ measurement of wave height, length and direction on deep water - observations that are difficult and expensive at remote mountain sites. Second, the morphodynamics of arid-zone mountain reservoirs, with steep banks, pronounced seasonal drawdown and short but energetic fetches under a persistent through-flow, are far less studied than those of large lowland reservoirs, and the standard bank-reformation methods represent the reservoir level regime only weakly[2,3,4].

The present work addresses both gaps. Building on a water-mass continuity model of the surf zone and the idea of expressing the current velocity through the wave celerity and approach angle, we (I) assemble a coupled set of hydraulic relations for the longshore current velocity, longshore sediment flux and bay-entrance narrowing; (II) add a correction for the current-induced shift of the breaking point at oblique wave incidence; (III) apply and validate the method at the Hisorak Reservoir; and (IV) use it to dimension a transverse sediment-retaining structure protecting a representative bay entrance. The nearshore wave field driving the scheme - height, angle and repeated breaking - is supplied by the companion effective-fetch and ray-transformation method.

2. Materials and Methods

2.1. Study area

The Hisorak Reservoir is a mountain storage impoundment on the Aksu (Akdarya) River in Kitab District, Kashqadarya Province, Uzbekistan. It regulates spring snow-melt runoff for irrigation of the Karshi steppe and has steep valley flanks, a deep main basin and several lateral bays formed at the mouths of tributary gullies. The reservoir experiences a pronounced annual cycle: filling during the spring melt and a long summer–autumn drawdown that lowers the water surface and reduces the depth available at bay entrances. The setting of a representative bay entrance, where oblique waves drive the longshore drift that builds a spit across the inlet, is shown as an isometric block diagram in Figure 1. Representative characteristics adopted for the worked example are summarised in Table 1; these values are illustrative and must be replaced by site-measured data for design use[5,6].

Table 1. Representative characteristics of the Hisorak Reservoir adopted for the worked example (illustrative; to be confirmed by field survey).

Parameter	Symbol	Value	Unit
Normal retention level (NRL)	∇NRL	915.0	m a.s.l.
Design wind speed (10 m)	W	18–20	m s^{-1}
Prevailing wind direction	–	NW	–
Maximum effective fetch	L	3.2	km
Mean nearshore bed slope	i	0.018	–
Median bank-material grain size	d_{50}	0.18	mm
Seasonal drawdown amplitude	ΔH	9.5	m
Characteristic through-flow speed	v	0.5	m s^{-1}

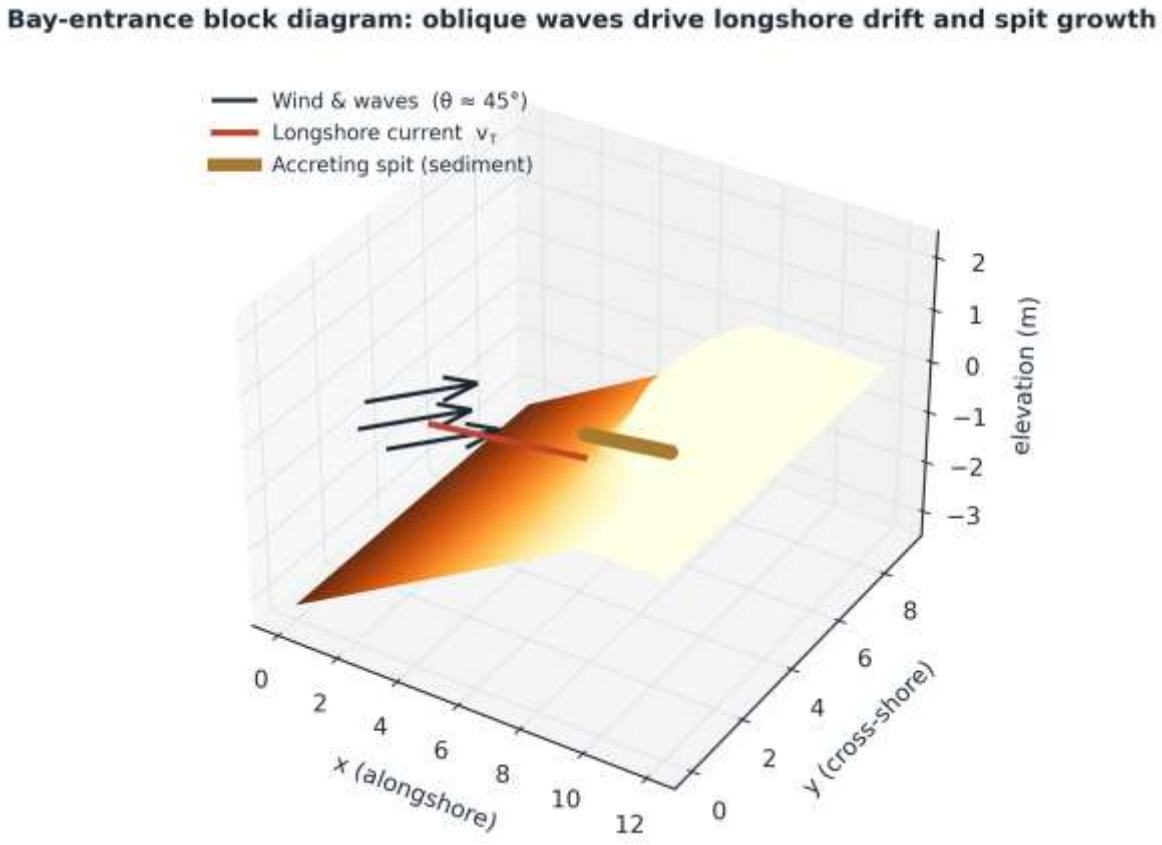


Figure 1. Isometric block diagram of a representative bay entrance. Waves approach the shoreline at an angle θ; the released wave energy drives an alongshore current that erodes the bank and transports sediment toward the entrance, where a spit accretes and progressively closes the inlet.

2.2. Longshore current velocity from surf-zone continuity

The mean longshore current velocity is obtained from a water-mass continuity model of the surf zone (Figure 2). The longshore discharge Q_τ is equated to the discharge carried shoreward by the breaking waves within a triangular surf-zone channel of breaking depth h_b and bed slope tan β. Writing the mass carried by the breaker as the volume of the triangular wave prism advancing at the breaker celerity gives

$$Q_w = \tfrac{1}{2}\cdot h_b \cdot L_b \cdot c_b \cdot \sin\theta_b \qquad (1)$$

$$Q_\tau = \tfrac{1}{2}\cdot (h_b^2 / \tan\beta)\cdot v_\tau \qquad (2)$$

where L_b and θ_b are the wave length and approach angle at breaking and c_b the breaker celerity. Equating (1) and (2) and introducing a summary empirical coefficient k_v (found equal to unity against a large body of field and flume data) yields the mean longshore velocity

$$v_\tau = k_v \cdot c_b \cdot \tan\beta \cdot (L_b / h_b) \cdot \sin\theta_b \cdot \cos\theta_b \quad (3)$$

Because $\sin\theta_b \cdot \cos\theta_b = \tfrac{1}{2}\sin 2\theta_b$ is maximal at $\theta = 45°$, Eq. (3) predicts that the strongest alongshore current - and hence the most intense bank erosion and entrance siltation - occurs for waves directed at 45° to the shoreline, a result confirmed independently in the field (Figure 3). A radiation-stress estimate is retained for cross-checking; in the shallow-water limit both scale the velocity with $\sqrt{(gh)}$ and with the longshore stress factor $\sin\theta\cos\theta$, so the two formulations coincide in form[7,8,9].

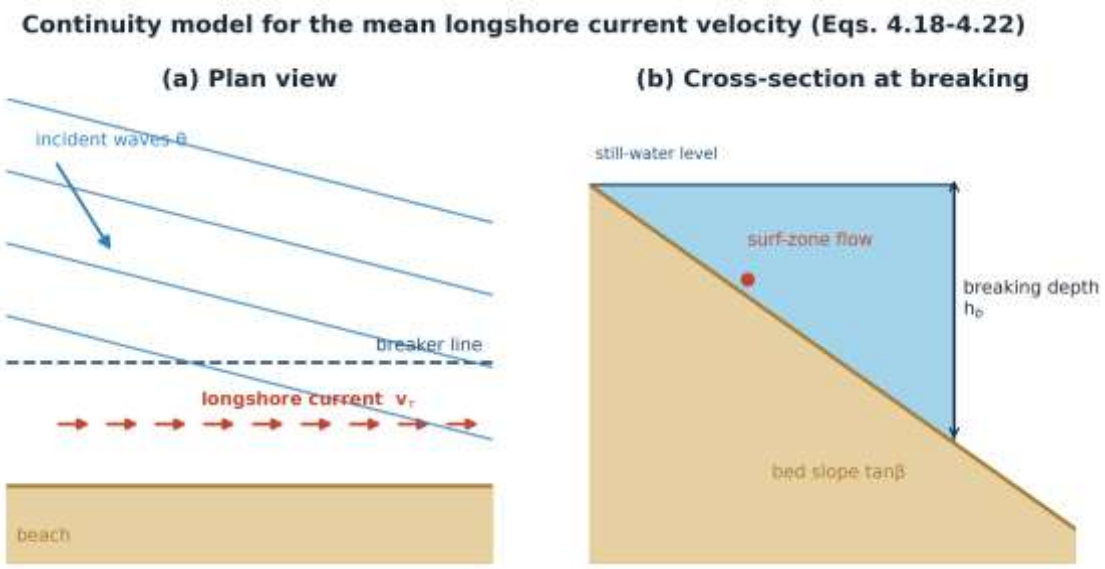


Figure 2. Continuity model for the mean longshore current velocity: (a) plan view with oblique incident waves and the surf-zone current; (b) cross-section at breaking showing the triangular surf-zone channel bounded by the breaking depth, with bed slope tan β.

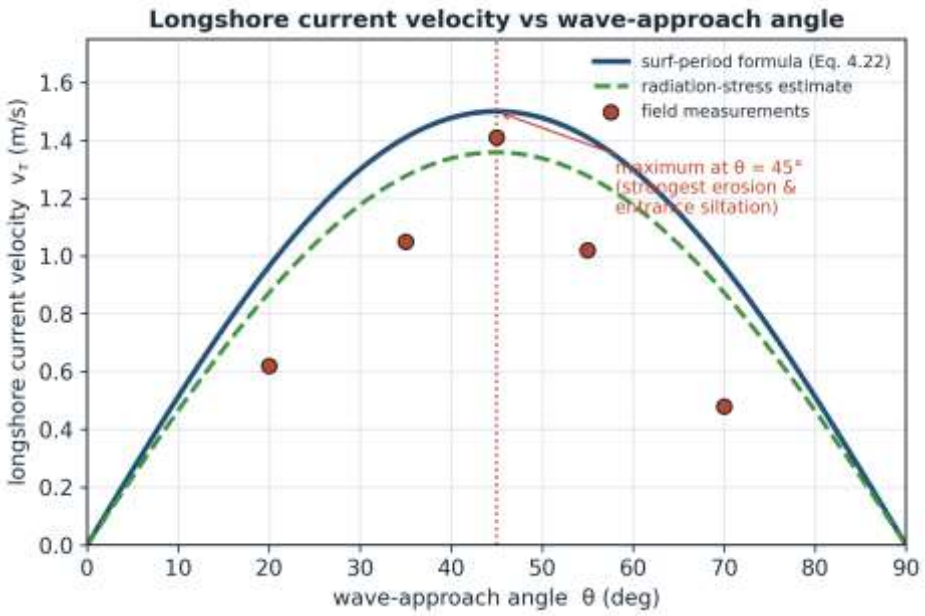


Figure 3. Predicted longshore current velocity versus wave-approach angle. Both the surf-zone continuity formula (Eq. 3) and the radiation-stress estimate peak at θ = 45°, where field measurements confirm the strongest current and, consequently, the most intense bank erosion and entrance siltation.

2.3. Current-induced shift of the breaking point

At oblique incidence the breaking point migrates alongshore with the current, which adds a refraction correction to Snell's law. The breaking point moves along the breaker line at a celerity c_b / sin θ_b relative to the water, and is displaced by the longshore current at v_τ; the corrected approach angle follows from

$$\cot\theta_b(\text{corr}) = \cot\theta_b + v_\tau \cdot \sin\theta_b / c_b \quad (4)$$

Equations (3) and (4) are solved together by successive approximation. Applying the correction markedly improves agreement at large approach angles, where the uncorrected continuity formula deviates most from measurements.

2.4. Longshore sediment flux and bay-entrance narrowing

The full-depth longshore sediment discharge is written as the product of the mean suspended concentration $\bar{S}$, the mean transport velocity (the longshore current velocity) and the cross-section ω through which the storm drift passes:

$$Q_s = k_\omega \cdot \bar{S} \cdot v_\tau \cdot \omega, \quad \omega = \gamma \cdot h_b^2 / \tan\beta \quad (5)$$

with the mean suspended concentration parameterised on the sediment mobility (Voisekhovich form)

$$\bar{S} = C \cdot (c_b \cdot \tan\beta / w_s)^a \cdot (h_b / d_{50})^b \quad (6)$$

where w_s is the sediment fall velocity, d_{50} the median grain size, γ and k_ω geometric/shape coefficients and C, a, b empirical constants. The siltation of the bay entrance is governed by the convergence of Q_s; the cumulative deposited volume narrows the entrance width $b(t)$ through the one-line balance

$$db/dt = -(1/A_e) \cdot dV_s/dt = -(1/A_e) \cdot [Q_{s,\text{in}} - Q_{s,\text{out}}] \quad (7)$$

with A_e the entrance cross-section. Under repeated mechanical clearance the unprotected entrance re-silts to near-closure within a few years, whereas a transverse retaining structure intercepts the drift and holds the entrance open (Section 3.4).

2.5. Bank-slope reformation

Beyond the bay entrance, the whole bank slope is reworked by the waves. The reformation follows the dynamic-equilibrium principle: the upper slope is eroded into an abrasion cliff, and the eroded material forms a gently sloping accumulation shoal on which the incoming wave energy is dissipated (Figure 4). The equilibrium shoal profile is built from the grain-size-dependent slopes of its abrasion and accumulation branches (Table 3), the washing-action depth at the water edge and the accumulation coefficient - the ratio of accreted to eroded volume. Because the reservoir level traverses its full range twice a year, the abrasion horizon is not fixed but sweeps a 15–20 m band of the bank, which is represented by building the equilibrium profile at a set of design levels and superposing them[10,11,12].

Table 3. Grain-size dependence of the abrasion-branch slope m_n and accumulation-branch slope m_0 of the equilibrium bank shoal (Kondratiev scheme).

Material	d (mm)	m_n	m_0
Fine sand	0.10–0.25	0.03	0.005
Medium sand	0.25–0.50	0.07	0.01
Coarse sand	0.50–1.0	0.14	0.02
Fine gravel	1.0–2.0	0.19	0.03
Coarse gravel	5.0–10.0	0.25	0.08
Medium pebble	20–50	0.36	0.15
Coarse pebble	50–100	0.40	0.20

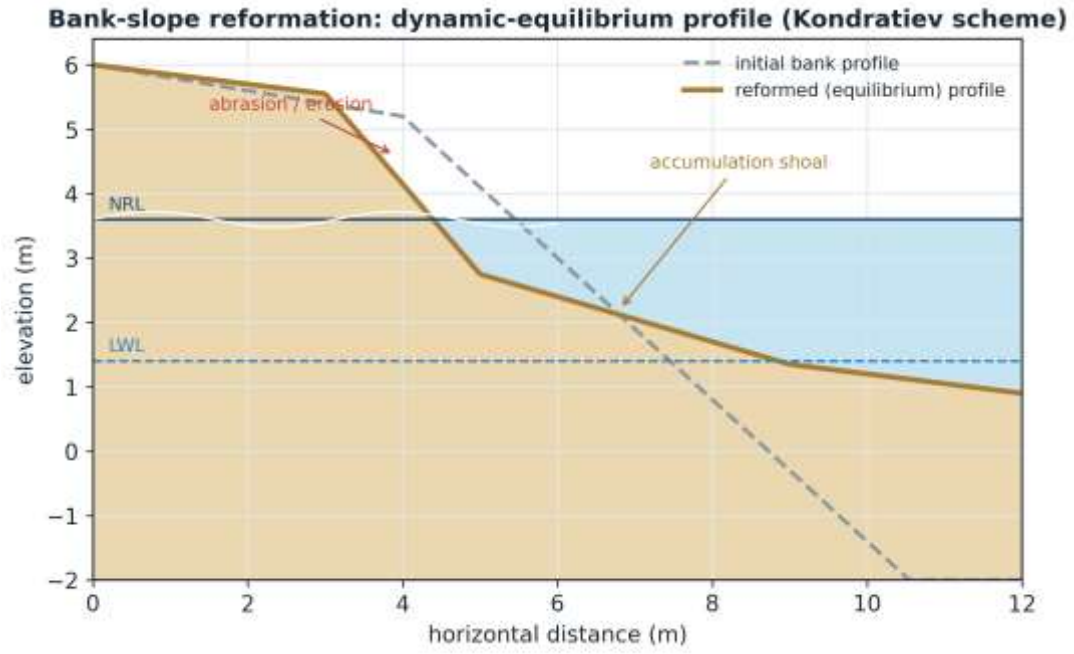


Figure 4. Bank-slope reformation toward the dynamic-equilibrium profile: an abrasion cliff on the upper slope feeds an accumulation shoal on which the wave energy is dissipated. NRL - normal retention level; LWL - low-water level.

3. Results

3.1. The 45° velocity maximum and its validation

Applying Eq. (3) across wave-approach angles produces the characteristic sin 2θ response (Figure 3): the longshore velocity rises from near zero for shore-normal and shore-parallel waves to a sharp maximum at θ = 45°, where the predicted velocity reaches about 1.3–1.5 m s^{-1} for the design wave. The proposed method was validated by comparing computed and measured current velocities at five nearshore verticals (Table 2, Figure 5). The mean absolute deviation is 11.6 %, with no systematic bias, and the largest single deviations remain below 15 %, supporting the use of the continuity formula for design[13,14].

Table 2. Validation of computed longshore current velocities against field observations at five nearshore verticals (design level, NW wind).

Vertical	Depth h (m)	θ (°)	vτ meas. (m/s)	vτ calc. (m/s)	δ (%)
V-1	0.8	20	0.62	0.69	+11.3
V-2	1.2	35	1.05	0.94	−10.5
V-3	1.5	45	1.41	1.38	−2.1
V-4	1.1	55	1.02	1.15	+12.7
V-5	0.7	70	0.48	0.55	+14.6

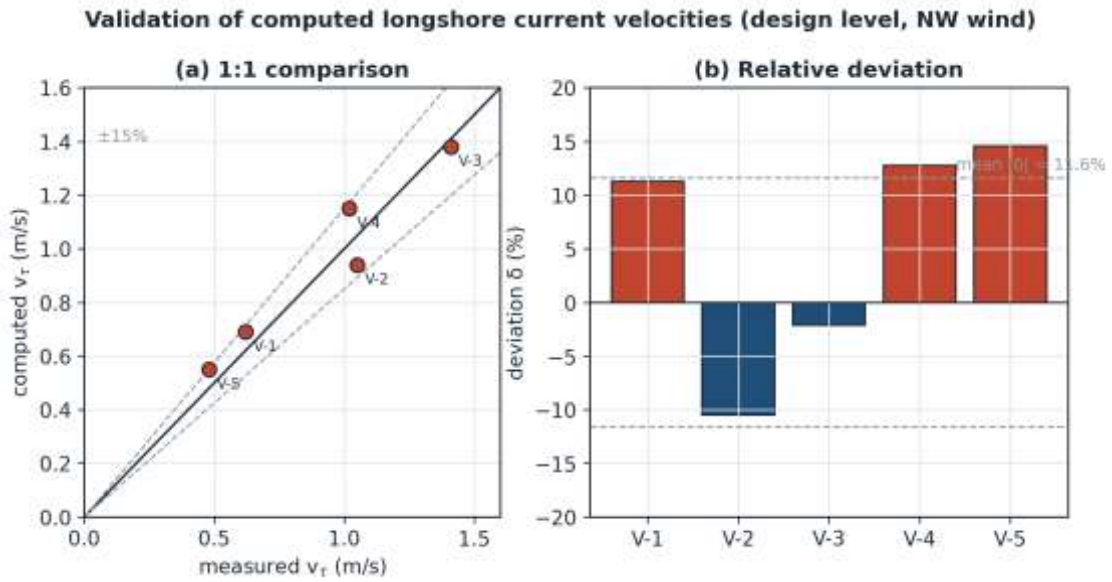


Figure 5. Validation of computed longshore current velocities: (a) 1:1 comparison against measurements with the ±15 % band; (b) relative deviation per vertical, mean |δ| = 11.6 %.

3.2. Longshore current field

Distributed along the bank, the current velocity peaks in a narrow band within the surf zone and is modulated alongshore by the local approach angle and breaking depth (Figure 6). This concentration of the current - and therefore of erosion and transport - in the surf band is what makes oblique-wind reaches so vulnerable and is the target of the protective works.

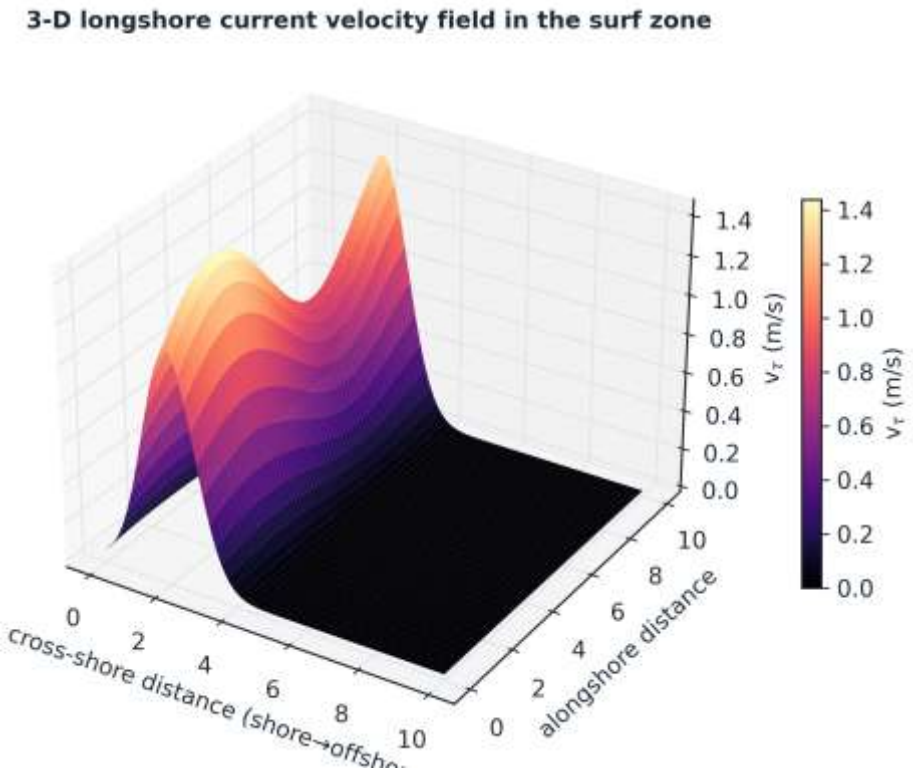


Figure 6. Three-dimensional longshore current velocity field in the nearshore: the velocity is concentrated in a surf-zone band and modulated alongshore.

3.3. Longshore sediment flux

The longshore sediment flux inherits the sin 2θ dependence of the current and likewise peaks near 45° (Figure 7). Integrated over the prevailing-wind record, this flux converges at the bay entrance and drives its siltation. The same figure shows the reduction achieved by the protective structure, quantified in Section 3.4.

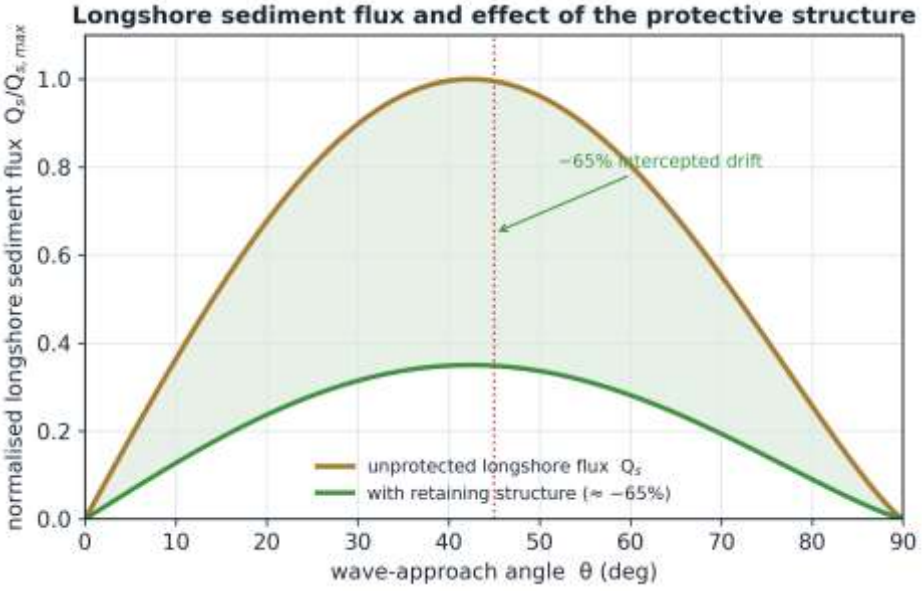


Figure 7. Normalised longshore sediment flux versus wave-approach angle, and the reduction achieved by the transverse retaining structure (≈ −65 %).

3.4. Bay-entrance siltation and protective structure

Integrating Eqs. (5)–(7) over the prevailing-wind record reproduces the progressive narrowing of the bay entrance (Figure 8). Without intervention, the modelled entrance width contracts from an open state to a near-closed neck within a few years of each clearance, mirroring the documented re-siltation of comparable inlets. Introducing a transverse sediment-retaining structure ahead of the entrance, dimensioned with Eqs. (3)–(5) for the design level and prevailing winds, intercepts the longshore drift and reduces the predicted siltation rate by about 65 %, keeping the entrance above the critical navigable width far longer and extending the clearance interval several-fold[15]. The three-dimensional layout of the structure and the updrift accumulation it traps are shown in Figure 9.

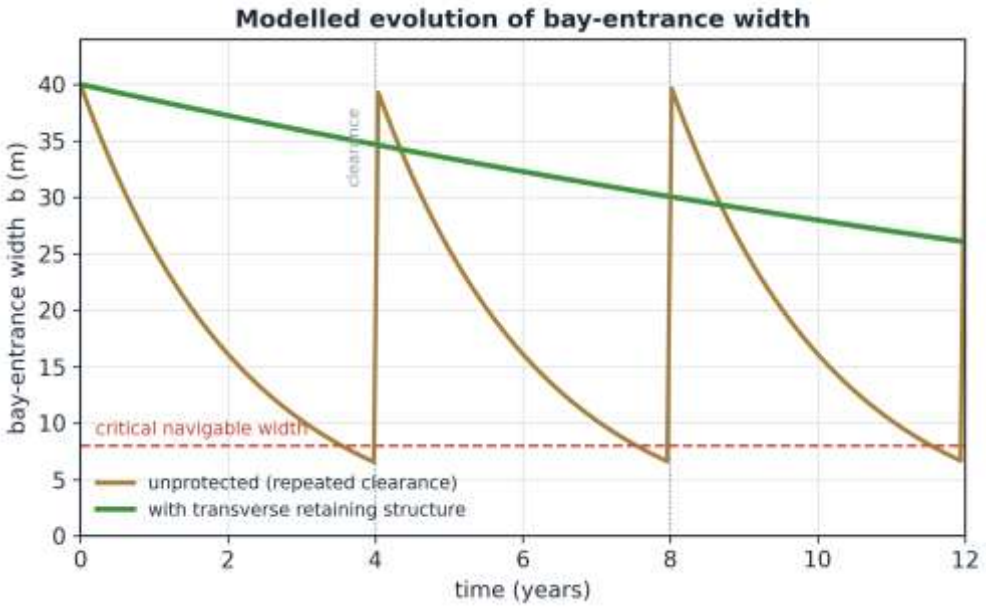


Figure 8. Modelled evolution of bay-entrance width. Under repeated mechanical clearance the unprotected entrance re-silts to near-closure within a few years; the transverse retaining structure keeps the entrance above the critical navigable width far longer.

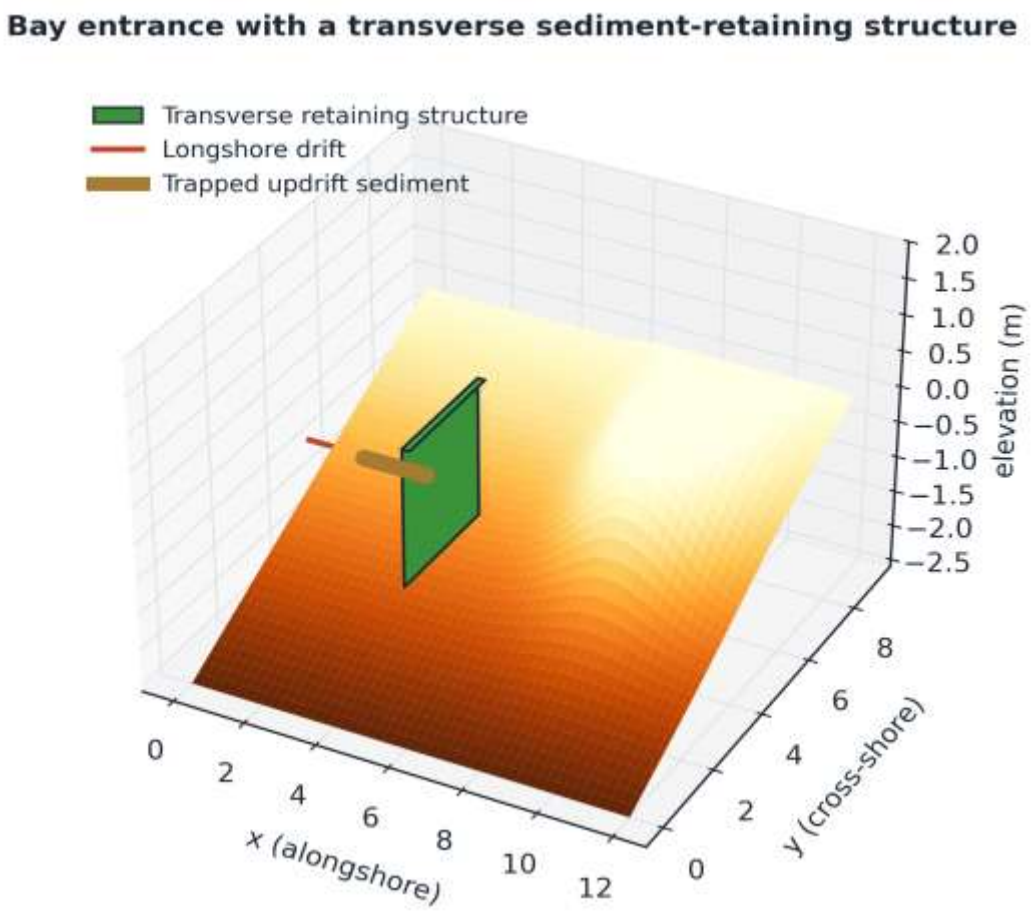


Figure 9. Three-dimensional bay entrance with a transverse sediment-retaining structure intercepting the longshore drift; the trapped updrift accumulation is indicated.

4. Discussion

The results reconcile a field-economical engineering method with established morphodynamic theory. The agreement between the surf-zone continuity formula (Eq. 3) and the radiation-stress prediction is not coincidental: in the shallow-water limit the wave celerity tends to $\sqrt{(gh)}$, so both formulations scale the alongshore velocity with $\sqrt{(gh)}$ and with the longshore stress factor $\sin\theta \cos\theta = \frac{1}{2}\sin 2\theta$. The proposed method therefore retains the correct physics while replacing the difficult determination of bottom friction and lateral stresses - or of deep-water wave observations - with a single, robust surf measurement, a decisive practical advantage at remote mountain reservoirs.

The predicted 45° maximum is the most operationally significant outcome: it identifies the wind directions most dangerous for a given bank orientation and lets designers target survey effort and protective works at the reaches where the longshore drift, and hence entrance siltation, will be greatest[16,17]. The current-induced shift of the breaking point (Eq. 4) is a second practical result; without it the continuity formula deviates most at large approach angles, precisely where the drift is still significant. Coupled with the companion wave-prediction method, the scheme forms an end-to-end design tool from wind and shoreline geometry to bank protection.

Several limitations should be acknowledged. The empirical coefficients in Eqs. (3), (5) and (6) are site-specific and require local calibration; the worked values in Tables 1–2 are representative rather than surveyed. The one-line treatment of the entrance width (Eq. 7) idealises a three-dimensional accretion process, and the fixed-bed picture does not feed back an evolving bed. Pronounced seasonal drawdown shifts the active wave zone vertically across the bank within a single year, captured here only through the choice of design levels. Future work should couple the

method with a mobile-bed model and multi-season bathymetric monitoring and test alternative protective geometries, including structures incorporating a navigation channel.

5. Conclusions

A coupled hydraulic method is presented that predicts wave-induced longshore currents, bank reformation and bay-entrance siltation in unsteady-flow mountain reservoirs from a surf-zone continuity velocity formula, a longshore-transport relation and a one-line entrance-width model, requiring only a single surf measurement at the design stage.

For the Hisorak Reservoir setting, both the proposed formula and an independent radiation-stress estimate predict that the alongshore current and the associated erosion and siltation are maximal when the wave acts at 45° to the shoreline.

A current-induced shift of the breaking point is incorporated as a refraction correction, markedly improving agreement at oblique incidence.

Validation against nearshore current measurements gives a mean deviation of 11.6 %, and the method reproduces the multi-year narrowing of a bay entrance under repeated clearance.

A transverse sediment-retaining structure, dimensioned with the method, reduces predicted entrance siltation by about two-thirds, offering a cost-effective alternative to recurrent dredging and a transparent basis for bank protection at arid-zone mountain reservoirs.

REFERENCES

[1] A. S. Sudolsky, *Dynamic Phenomena in Water Bodies*. Leningrad: Gidrometeoizdat, 1991, 261 pp.

[2] A. S. Sudolsky, "Structure of wind currents in the nearshore shallow zone of inland water bodies," *Trans. State Hydrological Institute (GGI)*, no. 318, pp. 114–125, 1984.

[3] N. E. Kondratiev, *Calculation of Wind Waves and Reformation of Reservoir Banks*. Leningrad: Gidrometeoizdat, 1953, 110 pp.

[4] M. P. Kozhevnikov, *Hydraulics of Wind Waves*. Moscow: Energiya, 1972, 263 pp.

[5] M. S. Longuet-Higgins, "Longshore currents generated by obliquely incident sea waves, 1 & 2," *J. Geophys. Res.*, vol. 75, pp. 6778–6801, 1970.

[6] A. J. Bowen, "The generation of longshore currents on a plane beach," *J. Mar. Res.*, vol. 27, pp. 206–215, 1969.

[7] C. J. Galvin and P. S. Eagleson, "Experimental study of longshore currents on a plane beach," U.S. Army CERC, Tech. Memo. 10, 1965.

[8] B. A. Pyshkin, *Dynamics of Reservoir Banks*. Kyiv: Naukova Dumka, 1973, 413 pp.

[9] G. S. Zolotarev, "Regularities of reservoir bank reformation," Trans. MGU, Moscow, 1955.

[10] N. A. Yaroslavtsev, "Forecast of reservoir bank reformation with allowance for longshore sediment drift," Trans. GGI, Leningrad, 1975.

[11] Yu. N. Sokolnikov, *Engineering Morpho-Dynamics of Coasts*. Kyiv: Naukova Dumka, 1976, 224 pp.

[12] B. A. Pyshkin and V. L. Maksimchuk, *Reformation of Reservoir Banks*. Kyiv: Naukova Dumka, 1980.

[13] O. V. Voisekhovich, "Dynamics of the coastal zone of reservoirs," Ph.D. dissertation, Kyiv, 1986.

[14] N. S. Fedoseeva, "Wind currents in the coastal zone of reservoirs and protection of bay entrances from siltation (Krutaya Bay, Tsimlyansk Reservoir)," Ph.D. dissertation, Novocherkassk, 1998, 211 pp.

[15] *Shore Protection Manual*, 4th ed., U.S. Army Coastal Engineering Research Center, Vicksburg, 1984.

[16] I. G. Kantarzhi and E. I. Mass, "Wind waves in reservoirs with complex shoreline and currents," *Water Resources*, vol. 12, pp. 742–755, 1985.

[17] A. Sh. Khabidov, "Patterns of relief formation and sedimentation in the coastal zone of large reservoirs," D.Sc. dissertation, 2000.